ISBN: 978-3-95450-231-8 ISSN: 2673-5490 doi: 10.18429/JACoW-IPAC2023-TUPM029

OPTIMIZATIONS OF A COMBINED RFQ COOLER PROTOTYPE FOR EXOTIC ION BEAMS

M. Cavenago*, C. Baltador, L. Bellan, M. Comunian, A. Galatà, M. Maggiore, A. Pisent, A. Ruzzon, INFN-LNL, Legnaro (PD), Italy; V. Variale, INFN-BA, Bari, Italy; F. Cavaliere, G. Maero, M. Romé, INFN-MI and Univ. Studi di Milano, Milano, Italy

Abstract

Cooling of secondary beams is often critical to accelerator based nuclear and sub-nuclear physics, with beams ranging from particle/anti-particle pairs (for the respective collider facilities) to exotic nuclei ions (like $^{132}Sn^{1+}$) as in the SPES (Selective Production of Exotic Species) project at LNL. A prototype of a radiofrequency quadrupole (RFQ) cooler (RFQC) was developed at LNL and is under test in the Eltrap facility at Milan University; Eltrap provides a solenoidal magnetic field. Typical limits of RFQC and high resolution mass spectrometer (HRMS) performances are recalled; HRMS requires less than 1 eV energy spread. The major RFQC parameters are reviewed, in particular for the case of Cs^+ against He gas, whose pressure ranges from 2 to 9 Pa; status of Milan test bench is updated, with some radiofrequency multiplexer and wiring details. Modeling and simulation results are summarized. Practical consideration on gas pumping are also included.

INTRODUCTION

Cooling [1, 2] of secondary beams is often necessary to their use in the context of accelerator based nuclear and sub-nuclear physics [3–6]. The case of exotic ion beams, as fostered by the LNL SPES project (Selective Production of Exotic Species) [7, 8], requires a very low emittance and cold beam for obtaining an adequate mass separation of isobaric ions, like for example $^{100}Tc^{+1}$ and $^{100}Nb^{+1}$; as a reference goal, the rms spread σ_E of ion kinetic energy K_i should be $\sigma_E^{out} \leq 0.5$ eVrms. Exotic nuclei are nuclei far from stability produced with fissions induced by a primary beam (proton 70 MeV) into a hot target, where these nuclei (with a distribution of nucleon A and atomic Z numbers) are stopped and neutralized; then they diffuse to an ion source IS1 [9, 10], where they are singly ionized and extracted as a beam, see Fig 1.a. The resulting beam energy spread [11, 12] depends of the used ion source (and from stability of the V_s source extraction voltage), say $\sigma_E^{in} \leq 5$ eVrms as a worst case for arc-based sources with $V_s \cong 40$ kV [10]. This spread is much lower than those observed for in-flight secondary particles manipulation [4], so that the exotic ion beam can be transported and cooled in linear traps, as the so-called Radio Frequency (RF) Quadrupole Coolers (RFQC); ion focusing is provided by the RF quadrupole.

In the RFQC, cooling (that is the reduction of the momentum variance of ion population) is due to an average effect of ion collisions with a lighter gas (typically Helium), in some ranges of ion speed or equivalently of the effective ion kinetic energy $K_i = m_i|\mathbf{v}|^2/2$ with m_i the ion mass and $\mathbf{v}$ the macromotion velocity [13, 14], that is, the ion velocity averaged over an RF period $\tau = 2\pi/\omega$. In SPES project, the beam (injected into and) extracted from an RFQC contains many exotic species, so that a HRMS (High Resolution Mass Separator) is needed. Inside RFQC, we also have beam diffusion (or straggling, due to harder collisions as in Fig. 1.b), which may heat a very cold beam (as discussed later) and increase the beam emittance; moveover beam emittance can grow for focusing mismatch, and for the effect of excessive RF fields. To better investigate this complex physics we thus install a test bench with a reduced size RFQC prototype in the Eltrap machine at Milano University, where also other linear traps (as Penning-Malmberg traps) for basic physics researches are studied [15, 16]; the test bench also helps to develop technical solutions in differential gas pumping and RF distribution as described in the following. Eltrap machine may also provide a solenoidal field B_z for additional ion focusing, with z the solenoid axis; $Oxyz$ be a Cartesian frame with O the solenoid center point and $Or\vartheta z$ be the cylindrical coordinates; as usual $r^2 = x^2 + y^2$. In Eltrap

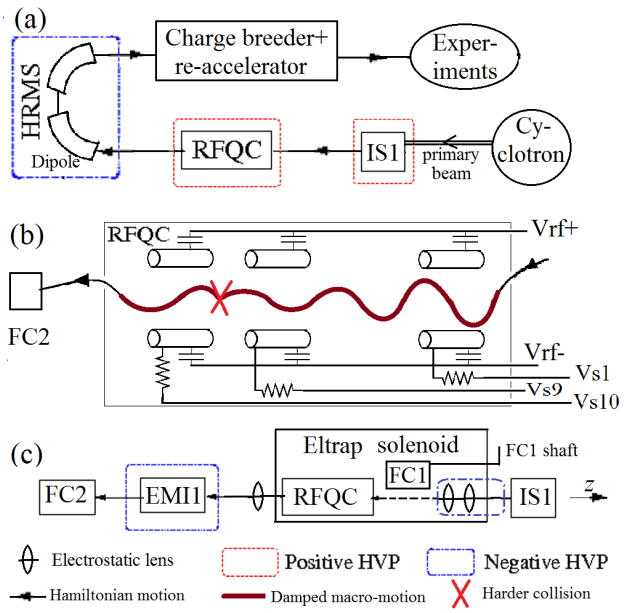

Figure 1: (a) relation of RFQC with the SPES project; (b) principle of RFQC confinement and cooling, with some electrodes, voltages and components shown; (c) the Eltrap machine RFQC installation, note emittance meter EMI1, ion source IS1 and Faraday cups FC1 and FC2.

* email address: cavenago@lnl.infn.it

ISBN: 978-3-95450-231-8 ISSN: 2673-5490 doi: 10.18429/JACoW-IPAC2023-TUPM029

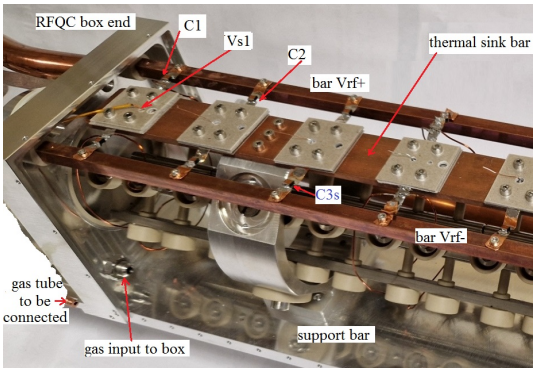

Figure 2: Detail of rf multiplexer (gas tight RFQC cover removed); the resistors are sandwiched between mica foils for heat disposal towards a large copper bar; capacitors as C1, C2 and C3s stay in He gas region.

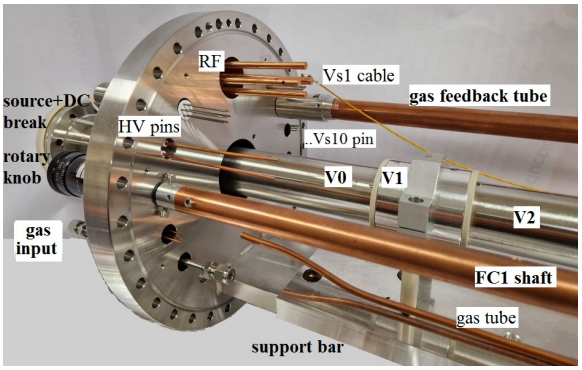

Figure 3: The plugin flange, seen from vacuum side, with one CF40 for redundant rf input pins, and 12 CF16 for other connection (as partly labeled); ion beam enter from drift tube V_0 connected to ion source IS1 and isolated from flange

ion diagnostic may be simplified because: 1) a lower input kinetic energy is used $K_i \leq 5$ keV; 2) the ion source is a commercial standardized surface ionization source, allowing several cathodes for K or Rb or Cs beams; 3) with current Cs cathode, we only have one ion species (namely $^{133}Cs^{+1}$); 4) transmission efficiency $\eta_t = I_2/I_1$ is simply verified, with I_1, I_2 the ion currents measured by Faraday cups FC1 (when inserted) and FC2, see Fig. 1.c.

PRINCIPLES AND ELTRAP RFQC SETUP

The RFQC [14, 17, 18] is enclosed in a box to maintain a He gas pressure from $p_g = 3$ Pa to 9 Pa, with beam in and exit holes as small as possible; let n_g and $T_g = 0.025$ eV be the gas density and temperature (in energy units). The RFQ rods are divided into N sections, so that different DC voltages V_i^s, $i = 1, \ldots, N$, can be applied to them with resistors $R \cong 0.5$ MΩ . The RF voltages V_{rf}^+ and V_{rf}^- in phase opposition are applied to quadrupole electrodes with capacitors C1; this multiplexer, placed in vacuum, with resistor sandwiched between mica foils for thermal dissipation see Fig. 2, allows to use only $N+2$ feed-through pins for driving $4N$ electrodes. The Eltrap solenoid vacuum chamber, 1.5 m long, 0.25 m inner diameter is a convenient ground reference; the RFQC prototype (with $N = 10$ sections in a gas tight box about 0.75 m long) is placed on the same bar as the beam injection optical elements, consisting in the drift tubes at voltages V_0, V_2 and V_4, the einzel lens at voltages V_1 and V_3 and the deceleration triode V_5, V_6 and V_7, housed in the antechamber A1. The extraction triode T_e (at voltages V_8, V_9 and V_{10}) and the antechamber A2 are cantilevered on the RFQC box. Feedtroughs for all these voltages stay on one single CF250 flange, see Fig. 3, so that these electrodes can be assembled outside the vacuum chamber, and form a single 'plug-in' module. Gas input, and the gauge monitoring p_g are also placed on this flange.

The emittance meter EMI1 and the final Faraday cup FC2, with their signal connections, are instead supported (see Figs. 2 and 3 in Ref [19]) by a CF200 4-way cross, with a septum (see Fig. 4) and a large turbopump TP550 on one side. Gas escaping RFQC box apertures is mostly collected by antechambers A1 and A2, connected with a network of 4 pipes (20 mm diameter) directly to this TP550 pump, with pipe conductance adjusted not to overload it. In other vacuum chamber regions, a pressure p_3 is maintained by a turbopump TP300; $p_3 < 10^{-5}$ Pa when RFQC is not in use.

For reference, source and transport voltages are here reported only for the 5 keV ion case. Then $V_0 = V_2 = V_4 = -4.8$ kV, which allow to use a precise $V_s = 200$ voltage on source emitter. By applying adequate drift voltages V_i^s (from 10 V to 100 V, with respect to RFQC box and Eltrap chamber) to the RFQC sections $i = 1, \ldots, N$, ions are first strongly decelerated at RFQC input, and then gently re-accelerated in the RFQC, arriving to RFQC box exit, where they are extracted. As sketched in Fig. 1.b, outside RFQC box, gas and RF are negligible, so the ion motion is simply Hamiltonian, but inside RFQC it is damped. For example, with e.g. $V_1^s = 100$ V, we have $K_i = e(V_s - V_1^s) = 100$ eV at RFQC input and $K_i^{10} = e(V_s - V_{10}^s) - \mathcal{E}_L$ at exit, with $\mathcal{E}_L$ the average energy loss [19]. In the ballistic regime, we plan to adjust V_{10}^s so that K_i^{10} is in the range [3, 10] eV; the trapped regime is defined by $K_i^{10} \cong 0$ eV, but this has the disadvantage that part of ions are stopped before exit, and transmission will decrease. On the contrary, in the ballistic regime almost all ions arrive at the RFQC exit, so that a goal $\eta_t \cong 0.9$ can be considered, apart from possible losses due to mismatches and RF heating. With plugin connection nearly complete, first beam transmission tests are expected within this Autumn, also depending on available rf amplifiers. Feedback control of p_g and protection of TP550 against gas overload also need experimental verification.

TRANSPORT AND COOLING SUMMARY

Writing the RF electric field as $\Re \mathbf{E}_f(\mathbf{x}) e^{i\omega t}$, the ponderomotive potential is $\phi_p = e|\mathbf{E}_f|^2/(4m_i\omega^2)$ with m_i the ion mass (and m_g be the gas mass). As a first approximation, we neglect micromotion , so that the only (time-averaged) effect of RF is to produce a ponderomotive force $\mathbf{F}_p \equiv e\mathbf{E}_p = -e\nabla\phi_p$. With V_{rf} the amplitude of RF voltage

ISBN: 978-3-95450-231-8 ISSN: 2673-5490 doi: 10.18429/JACoW-IPAC2023-TUPM029

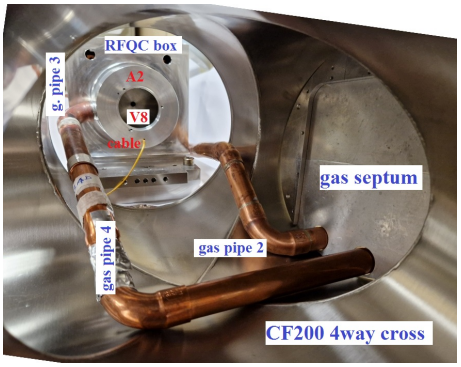

Figure 4: View of gas pipes and septum inside the 4way cross, with electrodes V9 and V10 dismounted from antechamber A2 to show V8 and its cable.

applied to electrodes with inner radius r_0 (that is, region $r \geq r_0$ contains the electrode rods), we have

$$\phi_p = \frac{m_i \omega_M^2 r^2}{2e}, \quad \omega_M = \frac{e\sqrt{2}}{m_i} \frac{|V_{rf}|}{\omega r_0^2}, \quad \Omega_i = \frac{e|\mathbf{B}^s|}{m_i}, \quad (1)$$

where ω_M and Ω_i are respectively the macromotion and cyclotron angular frequencies, with $\mathbf{B}^s$ the magnetostatic field (and $\mathbf{E}_s$ the electrostatic field). Each ion-gas collision changes the macromotion velocity $\mathbf{v}$ only slightly since $m_g/m_i \ll 1$ and $T_g < K_i$; in the statistical average, indicated with $\langle . \rangle$, the first order effect is a friction force $\mathbf{F}_r = -m_i \nu_i \mathbf{v}$ with $\nu_i(K_i)$ the momentum collision frequency. Second order is a straggling, which can be modeled by a Langevin equation

$$\mathrm{d}_t \mathbf{v} = \frac{e}{m_i} \left(\mathbf{E}_s + \mathbf{E}_p + \mathbf{v} \times \mathbf{B}^s \right) - \nu_i \mathbf{v} + \boldsymbol{\eta} \quad , \quad (2)$$

$$\langle \boldsymbol{\eta} \rangle = 0, \quad \langle \eta^m(t) \eta^n(t') \rangle = D^{mn} \delta(t - t') \quad , \quad (3)$$

where $\boldsymbol{\eta}$ is a random kick, with the second order moment given by the diffusion tensor D, and $m, n = 1, 2, 3$ or x, y, z are coordinate indexes.

In paraxial approximation $v_x \ll v_z$, calculating averages, we got $\nu_i = n_g f_1 |\mathbf{v}| \sigma_m$ and for example the component $D^{xx} = n_g f_1^2 |\mathbf{v}|^3 \sigma_{xx}$, with σ_m the momentum cross section [20–22], σ_{xx} the transverse diffusion cross section given in eq. 5 of Ref. [21] and $f_1 = m_g/(m_g + m_i)$. Let $\bar{v}$ be the solution of eq. 2 for $D = 0$, which can be calculated with the usual ray-tracing [19], and $\tilde{\mathbf{v}} = \mathbf{v} - \bar{\mathbf{v}}$ the fluctuation due to $\boldsymbol{\eta}$; also $\bar{\mathbf{x}} = \int \mathrm{d}t\, \bar{\mathbf{v}}$ and $\tilde{\mathbf{x}} = \mathbf{x} - \bar{\mathbf{x}}$. As an approximate and fast numerical method for eq. 2, consider a streamer or pencil P, that is the set of fluctuations around one single ray $\bar{\mathbf{x}}, \bar{\mathbf{v}}$; the evolution equations for the $\tilde{\mathbf{x}}, \tilde{\mathbf{v}}$ pencil 2nd order correlations can be written and solved in addition to the ray-tracing, verifying that $\langle \tilde{\mathbf{x}}^2 \rangle$ remains reasonable small ($\ll r_0$) in the same calculation [23], implemented by an extended leap-frog method and user scripts in a general matrix program [24], while axysymmetric field maps are imported from a multyphysics enviroment [25]. We use (also in full non-relativistic regime) the normalized emittance

$$\varepsilon_x^N = [\langle x^2 \rangle \langle p_x^2 \rangle - \langle x\, p_x \rangle^2]^{1/2} / (m_i c) \quad (4)$$

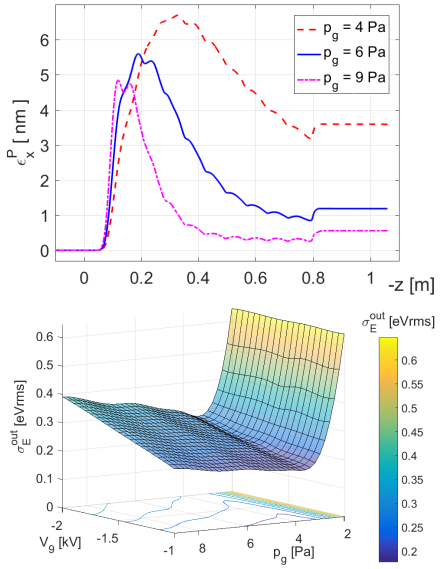

Figure 5: (a) pencil emittance evolution for several p_g and $V_p \equiv \phi_p(r_0) = 2$ V and adjusted $V_9 = -1.4$ kV; (b) output energy spread for initial $\sigma_E^{in} = 4$ rVms and several p_g, V_9

with $\mathbf{p}$ the ion momentum, and similarly for y; for axial symmetry we expect $\varepsilon_x^N \cong \varepsilon_y^N$. Invariant emittance ε_x^P of each single pencil P is similarly defined. The geometrical emittance $\varepsilon_x^g \cong c\varepsilon_x^N / v_z$ rapidly changes as v_z does, while pencil emittance changes are only due to collisions, as

$$\mathrm{d}_t (\epsilon_x^p)^2 = 2\langle x^2 \rangle D^{xx} - 2\nu_i (\epsilon_x^p)^2, \quad (5)$$

with the shorthand $\epsilon_x^p \cong c\varepsilon_x^P$; the emittance of all rays $\bar{\mathbf{v}}$ can be easily added to ε_x^P to get ε_x^N as a total. We may have $\varepsilon_x^N \in [0.3, 7] \times 10^{-9}$ m at ion source, and $\varepsilon_x^N \leq 3 \times 10^{-9}$ m is reachable at RFQC exit with $p_g > 5$ Pa.

Similarly, defining the transverse temperature as

$$T_t = m_i \langle \tilde{v}_x^2 + \tilde{v}_y^2 \rangle / 2, \quad (6)$$

we got an equilibrium value $T_t = m_i D^{xx} / \nu_i \gg T_g$, that is $T_t = 2 f_i K_i \sigma_{xx} / \sigma_i$, which shows the need of a low K_i[10]. In conclusion, results at different p_g are shown in fig 5, with ouput triode central voltage $V_9 = -1.4$ kV and ponderomotive net voltage $V_p = \phi_p(r_0) = 2$ V. Slightly lower ϵ_x^N are obtained with $V_p = 3$ V, that is $V_{rf} = 250$ V at a frequency $\omega/(2\pi) = 4$ MHz. Morover $\sigma_E^{out} < 0.5$ eVrms is achieved for a wide range $p_g > 3$ Pa.

ACKNOWLEDGEMENTS

Work partly supported by INFN-CSN5 (Technological Researches) under experiment Ion2neutral.

REFERENCES

[1] D. Larson, "Electron cooling at the SSC", *AIP Conf. Proc.*, vol. 326, p. 543, 1995. doi: 10.1063/1.47307

[2] S. van der Meer, AIP Conf. Proc. **153**, (1987) 1628

[3] R. H. Siemann, AIP Conf. Proc. **272**, (1992) 334

ISBN: 978-3-95450-231-8 ISSN: 2673-5490 doi: 10.18429/JACoW-IPAC2023-TUPM029

[4] D. Neuffer, "Principles and Applications of Muon Cooling", *Part. Accel.*, vol. 14, p. 75, 1983. doi: 10.2172/1156195

[5] H. Poth, "Electron cooling: Theory, experiment, application", *Phys. Reports*, vol. 196, p. 135, 1990. doi: 10.1016/0370-1573(90)90040-9

[6] G. de Angelis *et al.*, "The SPES Radioactive Ion Beam facility of INFN", *J. Phys.: Conf. Ser.*, vol. 580, p. (2015) 012014, 2015. doi: 10.1088/1742-6596/580/1/012014

[7] M. Comunian *et al.*, "Status of the SPES Exotic Beam Facility", *J. Phys.: Conf. Ser.* vol. 1401, p. 012002, 2020. doi: 10.1088/1742-6596/1401/1/012002

[8] G. Bisoffi *et al.*, "Progress in the design and construction of SPES at INFN-LNL", *Nucl. Instrum. Meth.*, vol. B376, 2016. doi: 10.1016/j.nimb.2016.01.024

[9] M. Maggiore *et al.*, "Plasma-beam traps and radiofrequency quadrupole beam coolers", *Rev. Sci. Instrum.*, vol. 85, p. 02B909, 2014. doi: 10.1063/1.4830357

[10] M. Manzolaro *et al.*, "Ongoing characterization of the forced electron beam induced arc discharge ion source for the selective production of exotic species facility", *Rev. Sci. Instrum.*, vol. 85, p. 02B918, 2014. doi: 10.1063/1.4857175

[11] M. Comunian, C. Baltador, L. Bellan, *et al.*, "Design of High Resolution Mass Spectrometer for SPES", in *Proc IPAC'18*, Vancouver, BC, Canada, 2018, p. 3252. doi: 10.18429/JACoW-IPAC2018-THPAK021

[12] M. Cavenago *et al.*, "Precision High Voltage Platform for Accelerators and Ion Mass Analysis", in *Proc. 29th ISDEIV*, online from Padova, Sep. 2021

[13] S. Schwarz, "IonCool-A versatile code to characterize gas-filled ion bunchers and coolers (not only) for nuclear physics applications", *Nucl. Instrum. Meth.*, vol. A566, p. 233, 2006. doi:10.1016/j.nima.2006.07.004

[14] R.B. Moore, O. Gianfrancesco, R. Lumbo, and S. Schwarz, "The use of high RFQ fields to manipulate ions", *Int. J. Mass Spectr.* vol. 251, p. 190, 2006. doi: 10.1016/j.ijms.2006.01.039

[15] G. Bettega *et al.*, Phys. Plasma 14, (2007) 102103

[16] C. Amsler *et al.*, Phys. Plasmas 29, 083303 (2022)

[17] M. Cavenago *et al.*, Rev. Sci. Instrum. **87** (2016) 02B504.

[18] R. Boussaid, G. Ban, G. Quémnér, Y. Merrer, and J. Lorry, "Development of a radio-frequency quadrupole cooler for high beam currents", *Phys. Rev. ST Aceel. Beams*, vol. 20, p. 124701, 2017. doi: 10.1103/PhysRevAccelBeams.20.124701

[19] M. Cavenago *et al.*, "Optimization of ion transport in a combined RFQ Cooler with axial magnetic Field", *Rev. Sci Instrum.*, vol. 90, p. 113334, 2019. doi: 10.1063/1.5128225

[20] M. A. Lieberman and A. J. Lichtenberg, *Principles of Plasma Discharges and Material Processing*, John Wiley, New York, 1994.

[21] M. Cavenago, C. Baltador, L. Bellan, *et al.*, Optimization of Mass Resolution Parameters combined with Ion Cooler Perfomance, 13th Int. Particle Acc. Conf. IPAC2022, Bangkok, Thailand, www.jacow.org, 2022, p. 2779.

[22] E.W. McDaniel and E.A. Mason, *The Mobility and Diffusion of Ions in Gases*, Wiley, New York, 1973.

[23] M. Cavenago *et al.*, "Optimization of ion transport in a combined RFQ Cooler with axial magnetic field", *J. Phys.: Conf. Ser.* vol. 2244, p. 012064, 2022. doi:10.1088/1742-6596/2244/1/012064

[24] *Matlab 2016a (TM)* or higher version, see also website http://www.mathworks.com

[25] *Comsol Multiphysics 3.5 (TM)* or higher version, see also http://www.comsol.eu